Published in final edited form as:
Neuroscience. 2011 February 3; 174: 50–63. doi:10.1016/j.neuroscience.2010.10.062.

COMPLEMENTARY SYNAPTIC DISTRIBUTION OF ENZYMES RESPONSIBLE FOR SYNTHESIS AND INACTIVATION OF THE ENDOCANNABINOID 2-ARACHIDONOYLGLYCEROL IN THE HUMAN HIPPOCAMPUS

A. Ludányi[a], **S. S.-J. Hu**[b], **M. Yamazaki**[c], **A. Tanimura**[d], **D. Piomelli**[e], **M. Watanabe**[f], **M. Kano**[d], **K. Sakimura**[c], **Z. Maglóczky**[a], **K. Mackie**[b], **T. F. Freund**[a], and **I. Katona**[a,*]

[a]Institute of Experimental Medicine, Hungarian Academy of Sciences, Budapest, H-1083, Szigony utca 43, Hungary

[b]Department of Psychological and Brain Sciences, Gill Center for Biomolecular Science, Indiana University, Bloomington, IN 47405, USA

[c]Department of Cellular Neurobiology, Brain Research Institute, Niigata University, Niigata 951-8585, Japan

[d]Department of Neurophysiology, Graduate School of Medicine, University of Tokyo, Tokyo 113-0033, Japan

[e]Department of Pharmacology, University of California, Irvine, California 92697-4625, USA

[f]Department of Anatomy, Hokkaido University School of Medicine, Sapporo 060-8638, Japan

Abstract

Clinical and experimental evidence demonstrates that endocannabinoids play either beneficial or adverse roles in many neurological and psychiatric disorders. Their medical significance may be best explained by the emerging concept that endocannabinoids are essential modulators of synaptic transmission throughout the central nervous system. However, the precise molecular architecture of the endocannabinoid signaling machinery in the human brain remains elusive. To address this issue, we investigated the synaptic distribution of metabolic enzymes for the most abundant endocannabinoid molecule, 2-arachidonoylglycerol (2-AG), in the postmortem human hippocampus. Immunostaining for diacylglycerol lipase-α (DGL-α), the main synthesizing enzyme of 2-AG, resulted in a laminar pattern corresponding to the termination zones of glutamatergic pathways. The highest density of DGL-α-immunostaining was observed in strata radiatum and oriens of the cornu ammonis and in the inner third of stratum moleculare of the dentate gyrus. At higher magnification, DGL-α-immunopositive puncta were distributed throughout the neuropil outlining the immunonegative main dendrites of pyramidal and granule cells. Electron microscopic analysis revealed that this pattern was due to the accumulation of DGL-α in dendritic spine heads. Similar DGL-α-immunostaining pattern was also found in hippocampi of wild-type, but not of DGL-α knockout mice. Using two independent antibodies developed against monoacylglycerol lipase (MGL), the predominant enzyme inactivating 2-AG, immunostaining also revealed a laminar and punctate staining pattern. However, as observed previously in rodent hippocampus, MGL was enriched in axon terminals instead of postsynaptic structures at the ultrastructural level. Taken together, these findings demonstrate the post- and presynaptic segregation of primary enzymes responsible for synthesis and elimination of 2-AG,

*Corresponding author. Tel: +36-1-2109400/267; fax: +36-1-2109412. katona@koki.hu (I. Katona).

respectively, in the human hippocampus. Thus, molecular architecture of the endocannabinoid signaling machinery supports retrograde regulation of synaptic activity, and its similar blueprint in rodents and humans further indicates that 2-AG's physiological role as a negative feed-back signal is an evolutionarily conserved feature of excitatory synapses.

Keywords

2-arachidonoylglycerol; diacylglycerol lipase; monoacylglycerol lipase; CB_1 cannabinoid receptor; glutamatergic synapse; hippocampus

Various preparations of the leaves, flowers and resinous extracts of the Cannabis plant have been consumed for both medical and recreational purposes since antiquity. Extensive research efforts aiming to explain the widespread therapeutic and behavioral effects evoked by Cannabis consumption finally led to the discovery of a new messenger system called the endocannabinoid system. It is composed of the CB_1 and CB_2 cannabinoid receptors (Devane et al., 1988; Matsuda et al., 1990; Munro et al., 1993), which are not only targets of the psychoactive compounds of the Cannabis plant, but more importantly, they are also activated by two endogenous lipid molecules produced by most cell types in the body (Devane et al., 1992; Mechoulam et al., 1995; Sugiura et al., 1995; Stella et al., 1997). The mobilization and elimination of these two endocannabinoid molecules called *N*-arachidonoylethanolamine (anandamide) and 2-arachidonoylglycerol (2-AG) are tightly regulated by surprisingly complex networks of metabolic enzymes and pathways in different cell types and tissues (Piomelli, 2003; Alexander and Kendall, 2007; Ahn et al., 2008). Following the clinical failure of brain-penetrating CB_1 receptor antagonists as therapeutics due to adverse psychiatric effects, the identification of novel molecular players regulating endocannabinoid levels has opened new possibilities, because drugs targeting these enzymes may have more selective actions (Ahn et al., 2009; Bisogno et al., 2009; Long et al., 2009; Solorzano et al., 2009). The wide spectrum of human neurological and psychiatric diseases in which the endocannabinoid system is implicated suggests a vast therapeutic potential (Mackie, 2006; Pacher et al., 2006; Katona and Freund, 2008). However, to take advantage of this potential requires full characterization of the enzymes regulating endocannabinoid signaling in the human brain.

A conceptual framework describing the major aspects of neuronal endocannabinoid signaling has emerged from the results of numerous animal studies in the last decade. In contrast to conventional neurotransmitters, endocannabinoids are primarily synthesized and released by postsynaptic neurons in an on-demand manner (Kreitzer and Regehr, 2001; Ohno-Shosaku et al., 2001; Wilson and Nicoll, 2001), and subsequently activate presynaptically located CB_1 cannabinoid receptors, thereby regulating neurotransmitter release from several types of axon terminals (Freund et al., 2003; Kano et al., 2009). This retrograde manner of synaptic endocannabinoid signaling is indispensable for various forms of homo- and heterosynaptic plasticity throughout the central nervous system (Chevaleyre et al., 2006; Kano et al., 2009), and probably accounts for the extensive involvement of the endocannabinoid system in brain disorders (Katona and Freund, 2008). Thus, molecular mechanisms regulating synaptic endocannabinoid signaling may be of pivotal importance in the therapeutic exploitation of the endocannabinoid system.

Although anandamide is the archetypical endocannabinoid molecule (Devane et al., 1992), and may tonically control presynaptic CB_1 receptors (Kim and Alger, 2010), most experimental evidence converge on the notion that 2-AG is the crucial retrograde messenger mediating on-demand forms of short- and long-term synaptic depression through CB_1 activation. Pharmacological inhibition of diacylglycerol lipase, including its alpha isoform

(DGL-α), the enzyme primarily responsible for 2-AG biosynthesis in adult brain (Bisogno et al., 2003), prevents retrograde endocannabinoid signaling in various experimental paradigms throughout the cerebral cortex (Chevaleyre and Castillo, 2003; Straiker and Mackie, 2005; Edwards et al., 2006, 2008; Lafourcade et al., 2007; Hashimotodani et al., 2008; Kellogg et al., 2009; Zhang et al., 2009, but see Min et al., 2010). Particularly compelling support for this concept also derives from the genetic inactivation of DGL-α, which completely abolishes endocannabinoid-mediated synaptic plasticity, for example in the hippocampus (Gao et al., 2010; Tanimura et al., 2010). Conversely, pharmacological blockade of monoacylglycerol lipase (MGL), the enzyme responsible for inactivation of the major fraction (~85%) of 2-AG in the brain (Dinh et al., 2002; Blankman et al., 2007), prolongs retrograde endocannabinoid signaling in distinct types of synapses (Makara et al., 2005; Hashimotodani et al., 2007; Lafourcade et al., 2007; Pan et al., 2009; Straiker et al., 2009; Straiker and Mackie, 2009; Zhang et al., 2009).

Widespread distribution of 2-AG in the human brain has recently been revealed (Palkovits et al., 2008) with a largely overlapping regional pattern to CB_1 receptors based on radioligand binding and *in situ* hybridization experiments (Herkenham et al., 1990; Westlake et al., 1994; Glass et al., 1997). Further high-resolution immunostaining and electron microscopic analysis in the human hippocampal formation and neocortex have narrowed down the presence of CB_1 receptors to GABAergic boutons (Katona et al., 2000; Eggan and Lewis, 2007; Ludanyi et al., 2008; Eggan et al., 2010; Magloczky et al., 2010) and also to glutamatergic axon terminals (Ludanyi et al., 2008). Together, these findings contribute to the hypothesis that 2-AG may be a synaptic messenger in the human nervous system. However, despite their potential therapeutic significance and their prominent mRNA expression levels in the human hippocampus (Ludanyi et al., 2008), the precise location of two key enzymes, DGL-α and MGL, known to regulate 2-AG signaling at chemical synapses in rodents have not yet been investigated in detail in the human brain. The aim of our study was therefore to uncover the precise molecular organization of the 2-AG signaling pathway at excitatory synapses in the human hippocampus by using novel antibodies with confirmed target specificity for DGL-α and MGL, as well as light and high-resolution electron microscopy.

EXPERIMENTAL PROCEDURES

Human tissue samples

Control hippocampi (n=5) were kindly provided by the Lenhossék Human Brain Program, Semmelweis University, Budapest. Control subjects (57±3 years) died suddenly from causes not directly involving any brain disease, and none of them had a history of any neurological disorders. The control subjects were processed for autopsy in the Department of Forensic Medicine of the Semmelweis University Medical School, Budapest, and the brains were removed 2–5 h after death. Informed consent was obtained for the use of brain tissue and for access to medical records for research purposes. Tissue was obtained and used in a manner compliant with the Declaration of Helsinki. All procedures were approved by the Regional and Institutional Committee of Science and Research Ethics of Scientific Council of Health (TUKEB 5-1/1996).

After postmortem removal, the hippocampal tissue was immediately dissected into 3- to 4-mm-thick blocks, and immersed in a fixative containing 4% paraformaldehyde, 0.1% glutaraldehyde, and 0.2% picric acid in phosphate buffer (PB; pH 7.4; 0.1 M). The blocks were first rinsed for 6 h at room temperature in the fixative, which was replaced every hour with a fresh solution. The blocks were then postfixed overnight in the same fixative solution, but without glutaraldehyde. In the case of one control brain, both the internal carotid and vertebral arteries were cannulated 4 h after death, and the brain was perfused with

physiological saline (2 L in 30 min) followed by a fixative solution containing 4% paraformaldehyde and 0.2% picric acid in PB (5 L in 3.5 h). The hippocampus was removed after perfusion, and was cut into 3- to 4-mm-thick blocks, and was postfixed in the same fixative solution overnight. Subsequently, 60-μm-thick coronal sections were prepared from the blocks with a Leica VTS-1000 Vibratome (Leica Microsystems, Wetzlar, Germany) for immunohistochemistry.

Mouse tissue samples

Adult male DGL-α knockout mice and wild-type littermates on C57BL/6 background (Tanimura et al., 2010) for the immunoperoxidase experiment as well as male wild-type C57BL/6 mice for the immunofluorescence experiment were perfused transcardially under deep pentobarbital (Phylaxia-Sanofi, Budapest, Hungary) anesthesia first with 0.9% saline and then with 4% paraformaldehyde dissolved in PB. After perfusion, the brain was removed from the skull, cut into 3- to 4-mm-thick blocks, and then 50-μm-thick coronal sections were sliced with a Leica VTS-1000 Vibratome for immunohistochemistry. Animal experiments were approved by the Committee of the Scientific Ethics of Animal Research (22.1/4027/003/2009), and were carried out according to institutional guidelines of ethical code and the Hungarian Act of Animal Care and Experimentation (1998. XXVIII. Section 243/1998).

Immunohistochemistry

Immunostaining of the slices was performed as described previously (Ludanyi et al., 2008). Briefly, after washing in PB (six times for 20 min each), sections were cryoprotected in 10% sucrose and in 30% sucrose in PB for 15 min and overnight, respectively, then freeze-thawed four times in an aluminium-foil boat over liquid nitrogen to enhance penetration of the antibodies without destroying the ultrastructure. Residual sucrose was washed from the tissue in PB (three times for 15 min) and then endogenous peroxidase activity was blocked for 10 min by treatment with 1% H_2O_2 dissolved in PB. Subsequently, all washing steps and antibody dilutions were carried out in Tris-buffered saline (TBS; pH 7.4; 0.05 M). After extensive washing in TBS (five times for 10 min each), sections were first blocked with 5% normal goat serum for 45 min, washed in PB for 15 min, and then incubated with the primary antibody of interest for 48 h. The following polyclonal, affinity-purified primary antibodies were used in the present study: rabbit anti-DGL-α (called “DGL-α-INT”; raised against residues 790–908 of the rat DGL-α protein; 1:1500–1:3000; Katona et al., 2006); rabbit anti-MGL (called “MGL-mid”; raised against residues 172–206 of the mouse MGL protein; 1:500–1:1000; Straiker et al., 2009); and rabbit anti-MGL (called “MGL-NT”; raised against residues 5–19 of the rat MGL protein; 1:3000; Dinh et al., 2002). The specificity of the DGL-α-INT antibody was confirmed by the lack of immunostaining in hippocampal sections derived from DGL-α knockout mice (Fig. 1B, D). The specificity of the two MGL antibodies was supported by immunostaining in HEK293 cells transiently expressing a V5 epitope-tagged MGL; by the lack of immunostaining in neurons pre-incubated with 5 μg/ml of the corresponding immunizing protein; and by the identical staining pattern in hippocampal sections at the electron microscopic level with the two antibodies raised against independent epitopes of the MGL protein (Dinh et al., 2002; Straiker et al., 2009).

After primary antibody incubation, human and mouse hippocampal sections were washed extensively in TBS (three times for 10 min each), then treated first with biotinylated goat anti-rabbit IgG (1:300; Vector Laboratories, Burlingame, CA, USA) for 2 h, washed again three times in TBS, and then incubated with avidin-biotinylated horseradish peroxidase complex (1:500; Elite-ABC; Vector Laboratories) for 1.5 h. This step was followed again by washing in TBS (twice for 20 min each) and in Tris buffer (TB, pH 7.6; twice for 20 min

each), and finally the immunoperoxidase reaction was developed using 3,3-diaminobenzidine (DAB; 0.3 mg/ml; Sigma, St. Louis, MO, USA) as chromogen and 0.01% H_2O_2 dissolved in TB. After the development of immunostaining, sections were washed in PB, treated with 1% OsO_4 in 0.1 M PB for 20 min, dehydrated in ascending series of ethanol and acetonitrile, and embedded in Durcupan (ACM; Fluka, Buchs, Switzerland). During dehydration, sections were also treated with 1% uranyl acetate in 70% ethanol for 20 min. After overnight incubation in Durcupan, the sections were mounted onto glass slides and coverslips were sealed by polymerization of Durcupan at 56 °C for 48 h. Light microscopic analysis of immunostaining was carried out with a Nikon Eclipse 80i upright microscope (Nikon Instruments Europe B.V., Amstelveen, The Netherlands), and light micrographs were taken with a DS-Fi1 digital camera (Nikon).

For electron microscopic investigations, selected immunoreactive profiles and regions (from stratum radiatum of the CA1 subfield and from stratum moleculare of the dentate gyrus) were photographed and re-embedded for further ultrathin sectioning. Series of consecutive ultrathin sections (60 nm) were collected on Formvar-coated single-slot grids and counterstained with lead citrate for 2 min. Electron micrographs were taken at 30,000–50,000× magnifications with a Hitachi 7100 electron microscope (Hitachi High-Technologies Corporation, Tokyo, Japan).

For immunofluorescence double staining, after freeze-thawing and intense washing, the sections were first blocked with 5% normal donkey serum for 45 min, and then incubated with mouse anti-NeuN (1:1000, Millipore, Billerica, MA, USA) and either with rabbit anti-DGL-α (1:1000), or rabbit anti-MGL (“MGL-mid”, 1:500), or rabbit anti-MGL (“MGL-NT”, 1:1000) primary antibodies for 48 h. Afterward, the sections were washed again in TBS three times for 15 min each, then incubated with secondary antibodies Alexa 594-conjugated goat anti-mouse IgG (1:400; Invitrogen, Carlsbad, CA, USA) and DyLight 488-conjugated donkey antirabbit IgG (1:400; Jackson Immuno Research, UK) for 2 h. Excess secondary antibody was washed out three times in TBS, and three times in 0.1 M PB for 15 min each. Finally, the sections were mounted in Vectashield (Vector Laboratories, Burlingame, CA, USA) onto glass slides, and the coverslips were sealed with nail polish. Image acquisition was performed with an inverted Nikon Eclipse Ti-E microscope equipped with an A1R confocal system (Nikon). Images of double labeling were obtained of a single focal plane by a 4× objective (NA 0.13) in sequential scanning mode using a four channel PMT detector.

For the adjustment of digital light and electron micrographs, Adobe Photoshop CS2 (Adobe Systems, San Jose, CA, USA) was used. In all imaging processes, adjustments (brightness and contrast) were done in the whole frame and no part of an image was modified separately in any way.

RESULTS

Distribution of DGL-α in the mouse and human hippocampus

To reveal the site of synthesis of the endocannabinoid 2-AG in the human hippocampus by determining the localization of its predominant synthesizing enzyme DGL-α (Bisogno et al., 2003; Gao et al., 2010; Tanimura et al., 2010), we first sought to identify an antibody with unequivocal specificity for this transmembrane serine hydrolase. Therefore, DGL-α-immunostaining was performed and compared in hippocampal sections derived from wild-type or DGL-α knockout mice (Tanimura et al., 2010). Using an affinity-purified antibody raised against a large intracellular loop on the C-terminus of DGL-α (“DGL-α INT”; Katona et al., 2006), immunoperoxidase reaction revealed at low magnification that the general dense distribution of DGL-α-immunostaining followed the topographic arrangement

of glutamatergic pathways in the wild-type hippocampus (Fig. 1A). In contrast, the immunoreactive material was almost fully absent in the DGL-α knockout hippocampus confirming the specificity of the "DGL-α INT" antibody (Fig. 1B, D). At higher magnification, the differences in staining intensity between the somatic and dendritic layers (the former receives exclusively GABAergic inputs, whereas the latter also contains abundant glutamatergic afferents) were even more pronounced (Fig. 1C). While nuclei and cell bodies in the principal cell layers were largely devoid of DGL-α-immunoreactivity, an intense punctate staining pattern was observed throughout the neuropil in those layers, which contain a high density of excitatory synapses in the hippocampus (e.g. in the stratum radiatum of the CA1 subfield, see Fig. 1C). This was in accordance with the observations we have reported earlier using this antibody in the hippocampus and in other regions (Katona et al., 2006; Matyas et al., 2008; Nyilas et al., 2009). On the other hand, this punctate labeling was largely missing in DGL-α knockout hippocampi (Fig. 1D).

Therefore, in the next set of experiments, we incubated hippocampal sections derived from human subjects together with hippocampal sections derived from wild-type C57BL/6 mice using the "DGL-α INT" antibody. At low magnification, immunofluorescence staining for DGL-α was unevenly distributed throughout the human hippocampal formation (Fig. 2D). This pattern followed the laminar organization of the hippocampus and was found to be largely similar in mice (Fig. 2A, D). At higher magnification, the highest density of DGL-α-immunoperoxidase reactivity was observed in the strata oriens and radiatum of the cornu ammonis (CA1–CA3) subfields, and in the inner molecular layer of the dentate gyrus (Fig. 3A, C), whereas somewhat weaker, but still significant density of DGL-α-immunoreactivity was found in the strata pyramidale and lacunosum-moleculare of the cornu ammonis and in the outer two-third of the stratum moleculare (Fig. 3A–C). Somata of pyramidal cells and dentate gyrus granule cells contained only very low amount of DGL-α-immunolabeling. At even higher magnification, the punctate staining pattern also showed striking similarities with the pattern observed in wild-type mice (Figs. 1C and 3B, D). This widespread granular pattern of DGL-α-immunoreactivity was visible throughout the hippocampal formation, but its distribution varied with regard to given subcellular profiles. For example, in the stratum radiatum of the CA1 subfield, DGL-α-positive granules were distributed along the main trunk of the apical dendrites of pyramidal cells, whereas the trunk itself was devoid of immunostaining (Fig. 3B). Similarly, apical and possibly oblique dendrites of granule cells also appeared to be outlined on their surface by dense DGL-α-immunolabeling (Fig. 3D).

Ultrastructural localization of DGL-α is largely confined to dendritic spine heads in the mouse and human hippocampus

To reveal the precise subcellular position of DGL-α in principal cells of the human hippocampus, we first tested the specificity of the "DGL-α INT" antibody at the ultrastructural level (Fig. 4A, B). Hippocampal sections from mice with different genotypes (wild-type and DGL-α knockout) were processed together within the same incubation wells to ensure identical treatment throughout the imunostaining procedure. Further high-resolution electron microscopic analysis in samples taken from the stratum radiatum of the CA1 subfield of wild-type hippocampus revealed that DGL-α-immunoreactivity was predominantly concentrated in dendritic spine heads receiving asymmetric, putative excitatory synapses, in accordance with previous findings (Katona et al., 2006; Yoshida et al., 2006) (Fig. 4A). Altogether, at least ~24% of dendritic spine heads were unequivocally positive for DGL-α immunoreactivity in our wild-type random samples (57 spines out of 238); this ratio should be treated as a conservative estimation restricted by epitope accessibility. In contrast, under identical staining condition, only two out of 201 spine heads (~1%) contained weak immunoperoxidase reaction end product in sections taken from the

DGL-α knockout mouse (Fig. 4B), indicating the low level of background in this immunostaining experiment.

To determine whether in the human hippocampus the same subcellular domain, namely the postsynaptic spine head, corresponds to the punctate staining pattern observed at the light microscopic level, hippocampal sections from human subjects (n=5) with DGL-α-immunostaining were also processed for further electron microscopic analysis. Two regions were selected for detailed investigations, the stratum radiatum of the CA1 region (Fig. 4C_1–C_2) and the inner third of the stratum moleculare of the dentate gyrus (Fig. 4D_1–D_2). In both regions, the DAB end product of the immunoperoxidase staining procedure, representing the subcellular position of DGL-α, was concentrated in dendritic spine heads protruding from DGL-α-immunonegative dendritic shafts. Because the majority of hippocampal GABAergic interneurons, including for example basket cells are aspiny, therefore the widespread occurrence of DGL-α in this characteristic subcellular compartment also reveals that principal cells express this enzyme in the human hippocampus. Notably, the DAB precipitate was consistently present within the spine heads through consecutive ultrathin sections. In contrast to this high concentration of DGL-α in dendritic spines, intensity of DGL-α-immunoreactivity did not reach the detection threshold in other subcellular profiles like excitatory and inhibitory axon terminals, or glial processes in the human hippocampus (Fig. 4C_1–D_2).

Taken together, these data ultimately confirm previous findings (Katona et al., 2006; Yoshida et al., 2006) that DGL-α accumulates postsynaptically in dendritic spines of principal cells in the mouse hippocampus and suggest that this 2-AG-synthesizing enzyme has a conserved function in the regulation of retrograde endocannabinoid signaling based on its entirely similar postsynaptic localization at excitatory synapses in the mouse and human hippocampus.

Distribution of MGL in the human hippocampus

If the enzyme responsible for 2-AG biogenesis is postsynaptically located (see above), whereas its receptor is presynaptically positioned (Ludanyi et al., 2008), then the next important question is where the 2-AG signal is terminated at excitatory synapses in the human hippocampus. Because MGL knockout mice have not yet become available to use as specificity controls, we employed two independent antibodies recognizing different epitopes of the MGL protein to characterize the regional distribution and subcellular localization of 2-AG's principal hydrolyzing enzyme, MGL (Dinh et al., 2002; Blankman et al., 2007; Straiker et al., 2009) in the human hippocampal formation.

Immunofluorescence staining for MGL using two different antibodies recognizing independent epitopes of the MGL protein (see Experimental Procedures) resulted in a comparable distribution pattern, although the general density of staining was stronger for the antibody "MGL-mid" in human hippocampal sections (Fig. 2B, E vs. C, F). Notably, as with the DGL-α-immunostaining, the distribution pattern of MGL mirrored the laminar structure of the hippocampal formation and was found to be similar in mouse and human hippocampi (Fig. 2B, C, E, F). At higher magnification, the stratum oriens showed the strongest density of MGL-immunoperoxidase reactivity in the cornu ammonis (Fig. 5A), but profound staining was also observed in strata pyramidale and radiatum (Fig. 5A, B). This pattern of expression in the three subfields of the cornu ammonis (CA1, CA2, and CA3) was very similar. Immunoperoxidase labeling for MGL was also found in the hilus and in the stratum moleculare of the dentate gyrus (Fig. 5C), with a somewhat stronger MGL-immunoreactivity visible in the outer two-thirds of the dentate molecular layer (Fig. 5C, D). Interestingly, this latter intensity pattern was in contrast with the distribution of DGL-α, which was more abundant in the inner third of the dentate molecular layer (note Figs. 3C

and 5C). At even higher magnification, cell bodies of pyramidal cells and granule cells were only weakly or not at all MGL-positive. Moreover, apical dendrites of pyramidal and granule cells were also largely devoid of immunolabeling for MGL (Fig. 5B, D). On the other hand, the neuropil among these dendrites and throughout the dendritic layers contained a dense, punctate MGL-positive staining. These varicosities were small, distributed with different densities in distinct layers and were often arranged in an array-like manner (Fig. 5D), reminiscent of the DGL-α-immunoreactivity pattern at the light microscopic level (Fig. 3B, D).

MGL is abundant in axon terminals forming asymmetric synapses in the human hippocampus

To test the prediction that the comparable dotted immunostaining pattern for DGL-α and MGL is due to the similar subcellular compartmentalization of these two enzymes with opposing functions in the metabolism of 2-AG, we performed a high-resolution electron microscopic analysis of MGL-immunostaining in the human hippocampal formation. The same regions were selected for detailed investigations as for DGL-α, the stratum radiatum of the CA1 region (Fig. 6A_1–B_2) and the inner third of stratum moleculare of the dentate gyrus (Fig. 6C_1–D_2).

Importantly, both antibodies revealed an identical staining pattern at the ultrastructural level. In addition, no differences in MGL-immunostaining were observed between strata radiatum and moleculare. At asymmetric, presumably glutamatergic synapses, MGL-immunoreactivity was restricted to presynaptic axon terminals, in contrast to the postsynaptic localization of DGL-α. These MGL-positive boutons terminated most often on dendritic spine heads, but occasionally dendritic shafts were also present among their postsynaptic targets. The DAB end product indicating the presence of the MGL protein was predominantly found in the central part of the axon terminals often close to synaptic vesicles and to active zone release sites (e.g. note b_2 in Fig. 6A_2 and b_2 in Fig. 6D_2), and could be consistently followed through consecutive ultrathin sections of the same terminals (Fig. 6). Besides the immunolabeling in axon terminals, MGL-immunoreactivity also appeared in thin axonal segments that could be often identified as preterminal axons through serial sections. In contrast to axonal profiles, consistent MGL-immunoreactivity confirmed with both antibodies remained under detection thresholds at postsynaptic sides, dendritic shafts, cell bodies and in glial processes.

Taken together, the abundance of MGL in axon terminals indicates that the majority of postsynaptically released 2-AG is inactivated presynaptically, close to its target, the CB_1 cannabinoid receptor. Moreover, together with similar findings in the rodent hippocampus (Gulyas et al., 2004), these data also suggest that the entire molecular architecture of retrograde 2-AG signaling at excitatory synapses is evolutionarily conserved across species.

DISCUSSION

Despite the compelling association of impaired endocannabinoid signaling with several neurological and psychiatric disorders (Pacher et al., 2006; Murray et al., 2007; Katona and Freund, 2008), our knowledge regarding the molecular architecture of endocannabinoid system in the human brain is still limited. In the present study, we provide evidence that (i) the enzymatic machinery responsible for the metabolism of the endocannabinoid 2-AG is also present in the human brain; (ii) its distribution follows the topographic layout of excitatory, glutamatergic pathways in the human hippocampal formation; (iii) and finally, its enzymes are restricted to complementary subcellular compartments at excitatory synapses. DGL-α, the key serine hydrolase in the biosynthesis of 2-AG (Bisogno et al., 2003; Gao et al., 2010; Tanimura et al., 2010) is found postsynaptically. In contrast, MGL, the primary

serine hydrolase responsible for hydrolyzing 2-AG (Dinh et al., 2002; Blankman et al., 2007) is localized presynaptically. Together with the presynaptic position of CB_1 cannabinoid receptors on glutamatergic axon terminals in the human hippocampus (Ludanyi et al., 2008), these data suggest that the molecular architecture of 2-AG signaling underlies 2-AG's postulated function as a retrograde synaptic messenger. Moreover, these findings also indicate that retrograde 2-AG signaling is an evolutionarily conserved feature of hippocampal excitatory synapses and its similar organization in rodents and humans may help to offer plausible strategies for human medical research based on experimental findings obtained in rodents.

Postsynaptic origin of 2-AG at glutamatergic synapses of the human hippocampus

An important implication of the present findings is the central role of DGL-α and 2-AG in the regulation of excitatory synaptic communication in the human hippocampus. Immunostaining for DGL-α at the light microscopic level resulted in an abundant punctate staining throughout the neuropil, which delineated the layered structure of the human hippocampal formation. On the other hand, characteristic profiles, like cell bodies and major dendritic trunks were weakly or not at all labeled. The granular pattern and its uneven, layered distribution suggest that DGL-α has a compartmentalized distribution at the subcellular level. The intense staining and its overlap with glutamatergic afferent pathways indicate that this compartment may be the glutamatergic synapse. Indeed, further electron microscopic examination revealed that DGL-α is exclusively found in postsynaptic spine heads receiving asymmetric, presumably excitatory glutamatergic synapses. This characteristic postsynaptic position was found both in stratum radiatum of the CA1 subfield and in stratum moleculare of the dentate gyrus. On the other hand, dendritic shafts from which these DGL-α-containing spines protrude, axon terminals and glial profiles were not consistently labeled suggesting that even if these subcellular domains hold low, at present undetectable, levels of the DGL-α enzyme, the majority of 2-AG biosynthesis occurs postsynaptically at glutamatergic synapses in the human hippocampal formation.

This peculiar subcellular position of DGL-α highlights its key function in the initiation of synaptic endocannabinoid signaling, whose human occurrence has been postulated based on numerous animal studies, but has never been demonstrated in human nervous tissue before. Using electron microscopy, a series of recent neuroanatomical findings reported a very similar postsynaptically compartmentalized distribution of DGL-α in several brain areas in rodents, for example in the prefrontal cortex (Lafourcade et al., 2007), in the hippocampus (Katona et al., 2006; Yoshida et al., 2006), in the striatum (Uchigashima et al., 2007), in the ventral tegmental area (Matyas et al., 2008), in the cerebellum (Yoshida et al., 2006), in the auditory brainstem (Zhao et al., 2009) and even in the dorsal horn of the spinal cord (Nyilas et al., 2009). Thus, we propose that the matching postsynaptic localization of DGL-α in the human hippocampus and in many rodent brain areas indicates that DGL-α is an evolutionarily conserved component of excitatory synapses and thereby its synaptic functions established in animal experiments can be extrapolated to the human brain as well.

What may be the synaptic function, which necessitates principal neurons to target DGL-α so precisely into dendritic spine heads? DGL-α synthesizes 2-AG from diacylglycerol, the common second messenger produced upon $G_{q/11}$-coupled receptor activation and phospholipase C-β (PLC-β) activity (Stella et al., 1997; Bisogno et al., 2003). The most abundant $G_{q/11}$-coupled receptor and PLC-β-type enzyme in hippocampal dendritic spine heads is the metabotropic glutamate receptor type 5 ($mGluR_5$) and PLC-β_1, respectively (Lujan et al., 1996; Fukaya et al., 2008), and indeed, activation of $mGluR_5$ leads to endocannabinoid-mediated retrograde synaptic suppression (Hashimotodani et al., 2005), and the elevation of 2-AG levels through PLC-β_1 and DGL-α activity (Jung et al., 2005, 2007). Because 2-AG inhibits glutamate release from excitatory nerve terminals in

hippocampal neurons (Straiker and Mackie, 2005; Bhaskaran and Smith, 2010), this negative feed-back pathway operating as a “synaptic circuit-breaker” may have a pivotal functional significance in controlling network excitability during neuronal insults leading to excitotoxicity (Katona and Freund, 2008).

Although the medical importance of such a protective messenger system is obvious, it is not yet clear if the same molecular machinery is functional at excitatory synapses of human neurons as well. The postsynaptic accumulation of DGL-α at excitatory synapses in human hippocampal samples described in the present study along with evidence that $mGluR_5$ is also present postsynaptically at excitatory synapses both in the human hippocampus (Tang et al., 2001) and in primate cortical areas (Muly et al., 2003) underlies this notion, though similar data are not yet available for PLC-βs in humans. Interestingly, an independent structural support derives from the striking similarity in the density of DGL-α and $mGluR_5$-immunostaining in relation to given hippocampal layers. For example, in the dentate gyrus, higher concentration of DGL-α was found in the inner third of the molecular layer than in the outer two-thirds of stratum moleculare both in rodents and in humans (see Fig. 3C in the present study), underlying the observation that excitatory inputs of granule cells received from mossy cells may be more tightly controlled by endocannabinoids than afferents from the entorhinal cortex (Chiu and Castillo, 2008). Similarly to DGL-α distribution, the density of $mGluR_5$-immunostaining is more pronounced in the inner molecular layer both in rodents (Shigemoto et al., 1997) and in humans (Blumcke et al., 1996). Finally, among glutamatergic terminal types, the concentration of CB_1 receptors is also highest in those arborizing in the inner molecular layer (Katona et al., 2006; Kawamura et al., 2006; Monory et al., 2006; Ludanyi et al., 2008). Whether this intensity difference reflects the higher density of excitatory synapses in the inner molecular layer both in rodents (Kaneko et al., 2002), and in humans (van der Hel et al., 2009) or it is due to synapse-specific variations in the regulation of synaptic 2-AG signaling needs to be established in further experiments. Nevertheless, the weaker density of MGL-immunostaining (see Fig. 5C) in the inner molecular layer indicating reduced capacity for 2-AG inactivation by MGL at mossy cell synapses gives some indirect support for the latter possibility and emphasizes that the termination of 2-AG signaling may be specifically regulated in the human hippocampus as well.

Presynaptic inactivation of 2-AG at glutamatergic synapses of the human hippocampus

We provide anatomical evidence that MGL, the main degrading enzyme of 2-AG has a widespread distribution in the human hippocampal formation. The nature of MGL-immunoreactivity was comparable to DGL-α-immunostaining at the light microscopic level, with the profuse punctate labeling covering the neuropil and outlining the laminar structure of the hippocampus. Electron microscopic analysis uncovered that this compartmentalized staining pattern is due to the accumulation of immunolabeling at excitatory synapses. However, in striking contrast to the postsynaptically localized DGL-α enzyme, MGL was present presynaptically in glutamatergic axon terminals. This anatomical observation is in agreement with previous findings obtained in the rodent hippocampus (Gulyas et al., 2004; Straiker et al., 2009), and it is also supported by recent physiological experiments demonstrating that MGL limits the duration of synaptic depression at hippocampal excitatory synapses (Pan et al., 2009; Straiker et al., 2009). In addition, although further immunohistochemical studies using antibodies with higher sensitivity may reveal that MGL is not fully restricted to glutamatergic synapses, the present findings indicate that the highest concentration of MGL protein is likely located in excitatory boutons in the human hippocampus.

MGL is the major degradative enzyme of 2-AG in the mouse brain. It is estimated that approximately 85% of the brain’s 2-AG hydrolysis activity is accounted for this serine

hydrolase (Blankman et al., 2007). Its widespread distribution in excitatory axon terminals in the human hippocampus suggests that MGL may also play a similarly important role in 2-AG hydrolysis in the human brain. Together with our previous findings demonstrating the ubiquitous presence of CB_1 cannabinoid receptors on the same excitatory terminals (Ludanyi et al., 2008), these data collectively corroborate that MGL is the key enzyme terminating synaptic 2-AG signaling after activation of presynaptic CB_1 receptors in the human hippocampal formation.

Given that acute *in vivo* administration of JLZ184, the most potent selective inhibitor of MGL currently available, replicates nearly all of the characteristic behavioral effects of Δ^9-tetrahydrocannabinol (Δ^9-THC) by protecting endogenously released 2-AG from degradation (Long et al., 2009), it is conceivable to hypothesize that JLZ184 may have a similar effect on the human brain based on the similar neuroanatomical localization of MGL in rodents and humans. Therefore, although MGL inhibitors hold great therapeutic potential in several medical applications (Saario and Laitinen, 2007), their predicted psychoactive side effects based on their cannabimimetic properties in animals (Long et al., 2009), should be taken into consideration when pondering the use of these compounds in humans.

CONCLUSION

These findings reveal the complementary post- and presynaptic segregation of DGL-α and MGL, the serine hydrolases primarily responsible for synthesis and elimination of 2-AG, respectively, in the human hippocampal formation. This synaptic distribution ideally supports retrograde regulation of neurotransmitter release by 2-AG via presynaptic CB_1 receptors. Moreover, its similarity in rodents and humans implies that the 2-AG signaling pathway may be an ancient, conserved trait of excitatory synapses.

Acknowledgments

This work was funded by the Hungarian Scientific Research Fund-Norwegian Financial Mechanism Joint Program (NNF 78918), European Research Council Grant 243153 and the János Bolyai scholarship to IK, by the Nemzeti Kutatási és Technológiai Hivatal (NKTH)-Országos Tudományos Kutatási Alapprogramok (OTKA) CNK77793 and European Union Contract LSHM-CT-2004-005166 to T.F.F., by the EPICURE FP6 EC LSHCT-2006-037315 grant to T.F.F. and Z.M., and by National Institutes of Health grants (DA09158, MH54671, NS030549) to T.F.F., and (DA011322, DA021696) to K.M. The authors wish to thank Mr. László Barna, the Nikon Microscopy Center at IEM, Nikon Austria GmbH and Auro-Science Consulting Ltd for kindly providing microscopy support. We are very grateful to Prof. Miklós Palkovits, Péter Sótonyi and Dr. Zsolt Borostyánkő i (Semmelweis University, Budapest, Hungary) for providing control human tissue. The excellent technical assistance of Dr. Eszter Horváth, Győző Goda, Katalin Iványi, Gabriella Katona-Urbán, Katalin Lengyel, Balázs Pintér and Emőke Szépné Simon is also acknowledged. We also thank Barna Dudok for his help in immunocytochemistry and preparation of figures, Virág Tresóné Takács for her help in electron microscopy and Drs. Rita Nyilas, Christopher Henstridge and Zsolt Lele for their comments on this manuscript.

Abbreviations

DAB	3,3-diaminobenzidine
DGL-α	diacylglycerol lipase-α
MGL	monoacylglycerol lipase
$mGluR_5$	metabotropic glutamate receptor type 5
PB	phosphate buffer
PLC-β	phospholipase C-β
TBS	tris-buffered saline

2-AG	2-arachidonoylglycerol
Δ^9-THC	Δ^9-tetrahydrocannabinol.

REFERENCES

Ahn K, Johnson DS, Mileni M, Beidler D, Long JZ, McKinney MK, Weerapana E, Sadagopan N, Liimatta M, Smith SE, Lazerwith S, Stiff C, Kamtekar S, Bhattacharya K, Zhang Y, Swaney S, Van Becelaere K, Stevens RC, Cravatt BF. Discovery and characterization of a highly selective FAAH inhibitor that reduces inflammatory pain. Chem Biol. 2009; 16:411–420. [PubMed: 19389627]

Ahn K, McKinney MK, Cravatt BF. Enzymatic pathways that regulate endocannabinoid signaling in the nervous system. Chem Rev. 2008; 108:1687–1707. [PubMed: 18429637]

Alexander SP, Kendall DA. The complications of promiscuity: endocannabinoid action and metabolism. Br J Pharmacol. 2007; 152:602–623. [PubMed: 17876303]

Bhaskaran MD, Smith BN. Cannabinoid-mediated inhibition of recurrent excitatory circuitry in the dentate gyrus in a mouse model of temporal lobe epilepsy. PLoS One. 2010; 5:e10683. [PubMed: 20498848]

Bisogno T, Burston JJ, Rai R, Allara M, Saha B, Mahadevan A, Razdan RK, Wiley JL, Di Marzo V. Synthesis and pharmacological activity of a potent inhibitor of the biosynthesis of the endocannabinoid 2-arachidonoylglycerol. Chem Med Chem. 2009; 4:946–950. [PubMed: 19266526]

Bisogno T, Howell F, Williams G, Minassi A, Cascio MG, Ligresti A, Matias I, Schiano-Moriello A, Paul P, Williams EJ, Gangadharan U, Hobbs C, Di Marzo V, Doherty P. Cloning of the first sn1-DAG lipases points to the spatial and temporal regulation of endocannabinoid signaling in the brain. J Cell Biol. 2003; 163:463–468. [PubMed: 14610053]

Blankman JL, Simon GM, Cravatt BF. A comprehensive profile of brain enzymes that hydrolyze the endocannabinoid 2-arachidonoylglycerol. Chem Biol. 2007; 14:1347–1356. [PubMed: 18096503]

Blumcke I, Behle K, Malitschek B, Kuhn R, Knopfel T, Wolf HK, Wiestler OD. Immunohistochemical distribution of metabotropic glutamate receptor subtypes mGluR1b, mGluR2/3, mGluR4a and mGluR5 in human hippocampus. Brain Res. 1996; 736:217–226. [PubMed: 8930327]

Chevaleyre V, Castillo PE. Heterosynaptic LTD of hippocampal GABAergic synapses: a novel role of endocannabinoids in regulating excitability. Neuron. 2003; 38:461–472. [PubMed: 12741992]

Chevaleyre V, Takahashi KA, Castillo PE. Endocannabinoid-mediated synaptic plasticity in the CNS. Annu Rev Neurosci. 2006; 29:37–76. [PubMed: 16776579]

Chiu CYQ, Castillo PE. Input-specific plasticity at excitatory synapses mediated by endocannabinoids in the dentate gyrus. Neuropharmacology. 2008; 54:68–78. [PubMed: 17706254]

Devane WA, Dysarz FA 3rd, Johnson MR, Melvin LS, Howlett AC. Determination and characterization of a cannabinoid receptor in rat brain. Mol Pharmacol. 1988; 34:605–613. [PubMed: 2848184]

Devane WA, Hanus L, Breuer A, Pertwee RG, Stevenson LA, Griffin G, Gibson D, Mandelbaum A, Etinger A, Mechoulam R. Isolation and structure of a brain constituent that binds to the cannabinoid receptor. Science. 1992; 258:1946–1949. [PubMed: 1470919]

Dinh TP, Carpenter D, Leslie FM, Freund TF, Katona I, Sensi SL, Kathuria S, Piomelli D. Brain monoglyceride lipase participating in endocannabinoid inactivation. Proc Natl Acad Sci U S A. 2002; 99:10819–10824. [PubMed: 12136125]

Edwards DA, Kim J, Alger BE. Multiple mechanisms of endocannabinoid response initiation in hippocampus. J Neurophysiol. 2006; 95:67–75. [PubMed: 16207781]

Edwards DA, Zhang L, Alger BE. Metaplastic control of the endocannabinoid system at inhibitory synapses in hippocampus. Proc Natl Acad Sci U S A. 2008; 105:8142–8147. [PubMed: 18523004]

Eggan SM, Lewis DA. Immunocytochemical distribution of the cannabinoid CB_1 receptor in the primate neocortex: a regional and laminar analysis. Cereb Cortex. 2007; 17:175–191. [PubMed: 16467563]

Eggan SM, Stoyak SR, Verrico CD, Lewis DA. Cannabinoid CB_1 receptor immunoreactivity in the prefrontal cortex: comparison of schizophrenia and major depressive disorder. Neuropsychopharmacology. 2010; 35:2060–2071. [PubMed: 20555313]

Freund TF, Katona I, Piomelli D. Role of endogenous cannabinoids in synaptic signaling. Physiol Rev. 2003; 83:1017–1066. [PubMed: 12843414]

Fukaya M, Uchigashima M, Nomura S, Hasegawa Y, Kikuchi H, Watanabe M. Predominant expression of phospholipase Cbeta1 in telencephalic principal neurons and cerebellar interneurons, and its close association with related signaling molecules in somatodendritic neuronal elements. Eur J Neurosci. 2008; 28:1744–1759. [PubMed: 18973591]

Gao Y, Vasilyev DV, Goncalves MB, Howell FV, Hobbs C, Reisenberg M, Shen R, Zhang MY, Strassle BW, Lu PM, Mark L, Piesla MJ, Deng KW, Kouranova EV, Ring RH, Whiteside GT, Bates B, Walsh FS, Williams G, Pangalos MN, Samad TA, Doherty P. Loss of retrograde endocannabinoid signaling and reduced adult neurogenesis in diacylglycerol lipase knock-out mice. J Neurosci. 2010; 30:2017–2024. [PubMed: 20147530]

Glass M, Dragunow M, Faull RLM. Cannabinoid receptors in the human brain: a detailed anatomical and quantitative autoradiographic study in the fetal, neonatal and adult human brain. Neuroscience. 1997; 77:299–318. [PubMed: 9472392]

Gulyas AI, Cravatt BF, Bracey MH, Dinh TP, Piomelli D, Boscia F, Freund TF. Segregation of two endocannabinoid-hydrolyzing enzymes into pre- and postsynaptic compartments in the rat hippocampus, cerebellum and amygdala. Eur J Neurosci. 2004; 20:441–458. [PubMed: 15233753]

Hashimotodani Y, Ohno-Shosaku T, Tsubokawa H, Ogata H, Emoto K, Maejima T, Araishi K, Shin HS, Kano M. Phospholipase Cbeta serves as a coincidence detector through its Ca2+ dependency for triggering retrograde endocannabinoid signal. Neuron. 2005; 45:257–268. [PubMed: 15664177]

Hashimotodani Y, Ohno-Shosaku T, Kano M. Presynaptic monoacylglycerol lipase activity determines basal endocannabinoid tone and terminates retrograde endocannabinoid signaling in the hippocampus. J Neurosci. 2007; 27:1211–1219. [PubMed: 17267577]

Hashimotodani Y, Ohno-Shosaku T, Maejima T, Fukami K, Kano M. Pharmacological evidence for the involvement of diacylglycerol lipase in depolarization-induced endocanabinoid release. Neuropharmacology. 2008; 54:58–67. [PubMed: 17655882]

Herkenham M, Lynn AB, Little MD, Johnson MR, Melvin LS, de Costa BR, Rice KC. Cannabinoid receptor localization in brain. Proc Natl Acad Sci U S A. 1990; 87:1932–1936. [PubMed: 2308954]

Jung KM, Astarita G, Zhu C, Wallace M, Mackie K, Piomelli D. A key role for diacylglycerol lipase-alpha in metabotropic glutamate receptor-dependent endocannabinoid mobilization. Mol Pharmacol. 2007; 72:612–621. [PubMed: 17584991]

Jung KM, Mangieri R, Stapleton C, Kim J, Fegley D, Wallace M, Mackie K, Piomelli D. Stimulation of endocannabinoid formation in brain slice cultures through activation of group I metabotropic glutamate receptors. Mol Pharmacol. 2005; 68:1196–1202. [PubMed: 16051747]

Kaneko T, Fujiyama F, Hioki H. Immunohistochemical localization of candidates for vesicular glutamate transporters in the rat brain. J Comp Neurol. 2002; 444:39–62. [PubMed: 11835181]

Kano M, Ohno-Shosaku T, Hashimotodani Y, Uchigashima M, Watanabe M. Endocannabinoid-mediated control of synaptic transmission. Physiol Rev. 2009; 89:309–380. [PubMed: 19126760]

Katona I, Freund TF. Endocannabinoid signaling as a synaptic circuit breaker in neurological disease. Nat Med. 2008; 14:923–930. [PubMed: 18776886]

Katona I, Sperlagh B, Magloczky Z, Santha E, Kofalvi A, Czirjak S, Mackie K, Vizi ES, Freund TF. GABAergic interneurons are the targets of cannabinoid actions in the human hippocampus. Neuroscience. 2000; 100:797–804. [PubMed: 11036213]

Katona I, Urban GM, Wallace M, Ledent C, Jung KM, Piomelli D, Mackie K, Freund TF. Molecular composition of the endocannabinoid system at glutamatergic synapses. J Neurosci. 2006; 26:5628–5637. [PubMed: 16723519]

Kawamura Y, Fukaya M, Maejima T, Yoshida T, Miura E, Watanabe M, Ohno-Shosaku T, Kano M. The CB_1 cannabinoid receptor is the major cannabinoid receptor at excitatory presynaptic sites in the hippocampus and cerebellum. J Neurosci. 2006; 26:2991–3001. [PubMed: 16540577]

Kellogg R, Mackie K, Straiker A. Cannabinoid CB_1 receptor-dependent long-term depression in autaptic excitatory neurons. J Neurophysiol. 2009; 102:1160–1171. [PubMed: 19494194]

Kim J, Alger BE. Reduction in endocannabinoid tone is a homeostatic mechanism for specific inhibitory synapses. Nat Neurosci. 2010; 13:592–600. [PubMed: 20348918]

Kreitzer AC, Regehr WG. Retrograde inhibition of presynaptic calcium influx by endogenous cannabinoids at excitatory synapses onto Purkinje cells. Neuron. 2001; 29:717–727. [PubMed: 11301030]

Lafourcade M, Elezgarai I, Mato S, Bakiri Y, Grandes P, Manzoni OJ. Molecular components and functions of the endocannabinoid system in mouse prefrontal cortex. Plos One. 2007; 2:e709. [PubMed: 17684555]

Long JZ, Li W, Booker L, Burston JJ, Kinsey SG, Schlosburg JE, Pavon FJ, Serrano AM, Selley DE, Parsons LH, Lichtman AH, Cravatt BF. Selective blockade of 2-arachidonoylglycerol hydrolysis produces cannabinoid behavioral effects. Nat Chem Biol. 2009; 5:37–44. [PubMed: 19029917]

Ludanyi A, Eross L, Czirjak S, Vajda J, Halasz P, Watanabe M, Palkovits M, Magloczky Z, Freund TF, Katona I. Downregulation of the CB_1 cannabinoid receptor and related molecular elements of the endocannabinoid system in epileptic human hippocampus. J Neurosci. 2008; 28:2976–2990. [PubMed: 18354002]

Lujan R, Nusser Z, Roberts JD, Shigemoto R, Somogyi P. Perisynaptic location of metabotropic glutamate receptors mGluR1 and mGluR5 on dendrites and dendritic spines in the rat hippocampus. Eur J Neurosci. 1996; 8:1488–1500. [PubMed: 8758956]

Mackie K. Cannabinoid receptors as therapeutic targets. Annu Rev Pharmacol. 2006; 46:101–122.

Magloczky Z, Toth K, Karlocai R, Nagy S, Eross L, Czirjak S, Vajda J, Rasonyi G, Kelemen A, Juhos V, Halasz P, Mackie K, Freund TF. Dynamic changes of CB_1-receptor expression in hippocampi of epileptic mice and humans. Epilepsia. 2010; 51:115–120. [PubMed: 20618415]

Makara JK, Mor M, Fegley D, Szabo SI, Kathuria S, Astarita G, Duranti A, Tontini A, Tarzia G, Rivara S, Freund TF, Piomelli D. Selective inhibition of 2-AG hydrolysis enhances endocannabinoid signaling in hippocampus. Nat Neurosci. 2005; 8:1139–1141. [PubMed: 16116451]

Matsuda LA, Lolait SJ, Brownstein MJ, Young AC, Bonner TI. Structure of a cannabinoid receptor and functional expression of the cloned cDNA. Nature. 1990; 346:561–564. [PubMed: 2165569]

Matyas F, Urban GM, Watanabe M, Mackie K, Zimmer A, Freund TF, Katona I. Identification of the sites of 2-arachidonoylglycerol synthesis and action imply retrograde endocannabinoid signaling at both GABAergic and glutamatergic synapses in the ventral tegmental area. Neuropharmacology. 2008; 54:95–107. [PubMed: 17655884]

Mechoulam R, Ben-Shabat S, Hanus L, Ligumsky M, Kaminski NE, Schatz AR, Gopher A, Almog S, Martin BR, Compton DR, Pertwee RG, Griffin G, Bayewitch M, Barg J, Vogel Z. Identification of an endogenous 2-monoglyceride, present in canine gut, that binds to cannabinoid receptors. Biochem Pharmacol. 1995; 50:83–90. [PubMed: 7605349]

Min R, Testa-Silva G, Heistek TS, Canto CB, Lodder JC, Bisogno T, Di Marzo V, Brussaard AB, Burnashev N, Mansvelder HD. Diacylglycerol lipase is not involved in depolarization-induced suppression of inhibition at unitary inhibitory connections in mouse hippocampus. J Neurosci. 2010; 30:2710–2715. [PubMed: 20164355]

Monory K, Massa F, Egertova M, Eder M, Blaudzun H, Westenbroek R, Kelsch W, Jacob W, Marsch R, Ekker M, Long J, Rubenstein JL, Goebbels S, Nave KA, During M, Klugmann M, Wolfel B, Dodt HU, Zieglgansberger W, Wotjak CT, Mackie K, Elphick MR, Marsicano G, Lutz B. The endocannabinoid system controls key epileptogenic circuits in the hippocampus. Neuron. 2006; 51:455–466. [PubMed: 16908411]

Muly EC, Maddox M, Smith Y. Distribution of mGluR1alpha and mGluR5 immunolabeling in primate prefrontal cortex. J Comp Neurol. 2003; 467:521–535. [PubMed: 14624486]

Munro S, Thomas KL, Abu-Shaar M. Molecular characterization of a peripheral receptor for cannabinoids. Nature. 1993; 365:61–65. [PubMed: 7689702]

Murray RM, Morrison PD, Henquet C, Di Forti M. Cannabis, the mind and society: the hash realities. Nat Rev Neurosci. 2007; 8:885–895. [PubMed: 17925811]

Nyilas R, Gregg LC, Mackie K, Watanabe M, Zimmer A, Hohmann AG, Katona I. Molecular architecture of endocannabinoid signaling at nociceptive synapses mediating analgesia. Eur J Neurosci. 2009; 29:1964–1978. [PubMed: 19453631]

Ohno-Shosaku T, Maejima T, Kano M. Endogenous cannabinoids mediate retrograde signals from depolarized postsynaptic neurons to presynaptic terminals. Neuron. 2001; 29:729–738. [PubMed: 11301031]

Pacher P, Batkai S, Kunos G. The endocannabinoid system as an emerging target of pharmacotherapy. Pharmacol Rev. 2006; 58:389–462. [PubMed: 16968947]

Palkovits M, Harvey-White J, Liu J, Kovacs ZS, Bobest M, Lovas G, Bago AG, Kunos G. Regional distribution and effects of postmortal delay on endocannabinoid content of the human brain. Neuroscience. 2008; 152:1032–1039. [PubMed: 18343585]

Pan B, Wang W, Long JZ, Sun DL, Hillard CJ, Cravatt BF, Liu QS. Blockade of 2-arachidonoylglycerol hydrolysis by selective monoacylglycerol lipase inhibitor4-nitrophenyl 4-(dibenzo[d][1,3] dioxol-5-yl(hydroxy)methyl) piperidine-1-carboxylate (JZL184) enhances retrograde endocannabinoid signaling. J Pharmacol Exp Ther. 2009; 331:591–597. [PubMed: 19666749]

Piomelli D. The molecular logic of endocannabinoid signalling. Nat Rev Neurosci. 2003; 4:873–884. [PubMed: 14595399]

Saario SM, Laitinen JT. Therapeutic potential of endocannabinoid-hydrolysing enzyme inhibitors. Basic Clin Pharmacol Toxicol. 2007; 101:287–293. [PubMed: 17910610]

Shigemoto R, Kinoshita A, Wada E, Nomura S, Ohishi H, Takada M, Flor PJ, Neki A, Abe T, Nakanishi S, Mizuno N. Differential presynaptic localization of metabotropic glutamate receptor subtypes in the rat hippocampus. J Neurosci. 1997; 17:7503–7522. [PubMed: 9295396]

Solorzano C, Zhu C, Battista N, Astarita G, Lodola A, Rivara S, Mor M, Russo R, Maccarrone M, Antonietti F, Duranti A, Tontini A, Cuzzocrea S, Tarzia G, Piomelli D. Selective N-acylethanolamine-hydrolyzing acid amidase inhibition reveals a key role for endogenous palmitoylethanolamide in inflammation. Proc Natl Acad Sci U S A. 2009; 106:20966–20971. [PubMed: 19926854]

Stella N, Schweitzer P, Piomelli D. A second endogenous cannabinoid that modulates long-term potentiation. Nature. 1997; 388:773–778. [PubMed: 9285589]

Straiker A, Hu SSJ, Long JZ, Arnold A, Wager-Miller J, Cravatt BF, Mackie K. Monoacylglycerol lipase limits the duration of endocannabinoid-mediated depolarization-induced suppression of excitation in autaptic hippocampal neurons. Mol Pharmacol. 2009; 76:1220–1227. [PubMed: 19767452]

Straiker A, Mackie K. Depolarization-induced suppression of excitation in murine autaptic hippocampal neurones. J Physiol (London). 2005; 569:501–517. [PubMed: 16179366]

Straiker A, Mackie K. Cannabinoid signaling in inhibitory autaptic hippocampal neurons. Neuroscience. 2009; 163:190–201. [PubMed: 19501632]

Sugiura T, Kondo S, Sukagawa A, Nakane S, Shinoda A, Itoh K, Yamashita A, Waku K. 2-Arachidonoylglycerol: a possible endogenous cannabinoid receptor ligand in brain. Biochem Biophys Res Commun. 1995; 215:89–97. [PubMed: 7575630]

Tang FR, Lee WL, Yeo TT. Expression of the group I metabotropic glutamate receptor in the hippocampus of patients with mesial temporal lobe epilepsy. J Neurocytol. 2001; 30:403–411. [PubMed: 11951051]

Tanimura A, Yamazaki M, Hashimotodani Y, Uchigashima M, Kawata S, Abe M, Kita Y, Hashimoto K, Shimizu T, Watanabe M, Sakimura K, Kano M. The endocannabinoid 2-arachidonoylglycerol produced by diacylglycerol lipase alpha mediates retrograde suppression of synaptic transmission. Neuron. 2010; 65:320–327. [PubMed: 20159446]

Uchigashima M, Narushima M, Fukaya M, Katona I, Kano M, Watanabe M. Subcellular arrangement of molecules for 2-arachidonoyl-glycerol-mediated retrograde signaling and its physiological contribution to synaptic modulation in the striatum. J Neurosci. 2007; 27:3663–3676. [PubMed: 17409230]

van der Hel WS, Verlinde SA, Meijer DH, de Wit M, Rensen MG, van Gassen KL, van Rijen PC, van Veelen CW, de Graan PN. Hippocampal distribution of vesicular glutamate transporter 1 in patients with temporal lobe epilepsy. Epilepsia. 2009; 50:1717–1728. [PubMed: 19389151]

Westlake TM, Howlett AC, Bonner TI, Matsuda LA, Herkenham M. Cannabinoid receptor binding and messenger RNA expression in human brain: an *in vitro* receptor autoradiography and *in situ* hybridization histochemistry study of normal aged and Alzheimer's brains. Neuroscience. 1994; 63:637–652. [PubMed: 7898667]

Wilson RI, Nicoll RA. Endogenous cannabinoids mediate retrograde signalling at hippocampal synapses. Nature. 2001; 410:588–592. [PubMed: 11279497]

Yoshida T, Fukaya M, Uchigashima M, Miura E, Kamiya H, Kano M, Watanabe M. Localization of diacylglycerol lipase-alpha around postsynaptic spine suggests close proximity between production site of an endocannabinoid, 2-arachidonoyl-glycerol, and presynaptic cannabinoid CB_1 receptor. J Neurosci. 2006; 26:4740–4751. [PubMed: 16672646]

Zhang SY, Xu M, Miao QL, Poo MM, Zhang XH. Endocannabinoid-dependent homeostatic regulation of inhibitory synapses by miniature excitatory synaptic activities. J Neurosci. 2009; 29:13222–13231. [PubMed: 19846710]

Zhao Y, Rubio ME, Tzounopoulos T. Distinct functional and anatomical architecture of the endocannabinoid system in the auditory brainstem. J Neurophysiol. 2009; 101:2434–2446. [PubMed: 19279154]

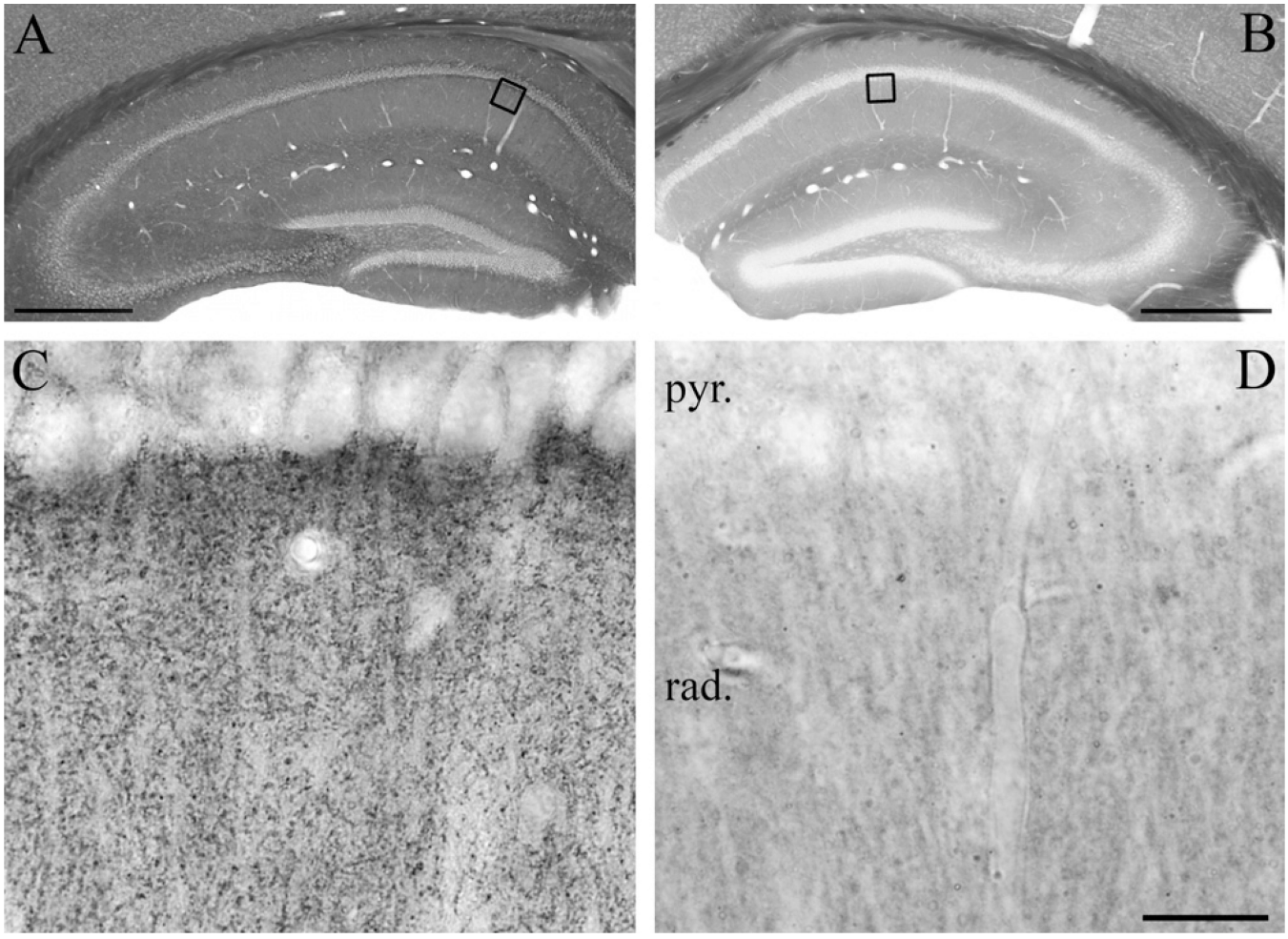

Fig. 1.

Confirmation of the specificity of the "DGL-α-INT" antibody in DGL-α knockout mice. (A) Immunostaining in wild-type mice using an antibody raised against a 118 residue-long intracellular segment of the DGL-α protein visualizes the layered structure of the hippocampus. The dendritic layers contain high density of DGL-α immunoreactivity, whereas the somatic layers stand out as DGL-α immunonegative. (B) In contrast, immunostaining in the hippocampus of a DGL-α knockout mouse shows no similar immunoreactive profiles, demonstrating antibody specificity. The sections presented in (A) and (B) were incubated in parallel throughout the immunostaining and dehydration procedures to ensure unequivocal comparison. Note the similar intensity of dark tone in the white matter generated by osmification, which confirms identical treatment. Open boxes denote the positions of corresponding insets in the CA1 subfield (C in A, D in B). (C) At higher magnification, immunoreactivity for DGL-α covers the stratum radiatum in wild-type mice. The characteristic punctate staining outlines the major apical trunk of pyramidal cell dendrites, which along with pyramidal cell somata are largely devoid of DGL-α immunoreactivity. (D) The dense DGL-α immunopositive staining in the neuropil is absent in the hippocampus of DGL-α knockout mice. Abbreviations: rad, stratum radiatum; pyr, stratum pyramidale. Scale bars: (A–B) 500 μm; (C–D, shown in D) 20 μm.

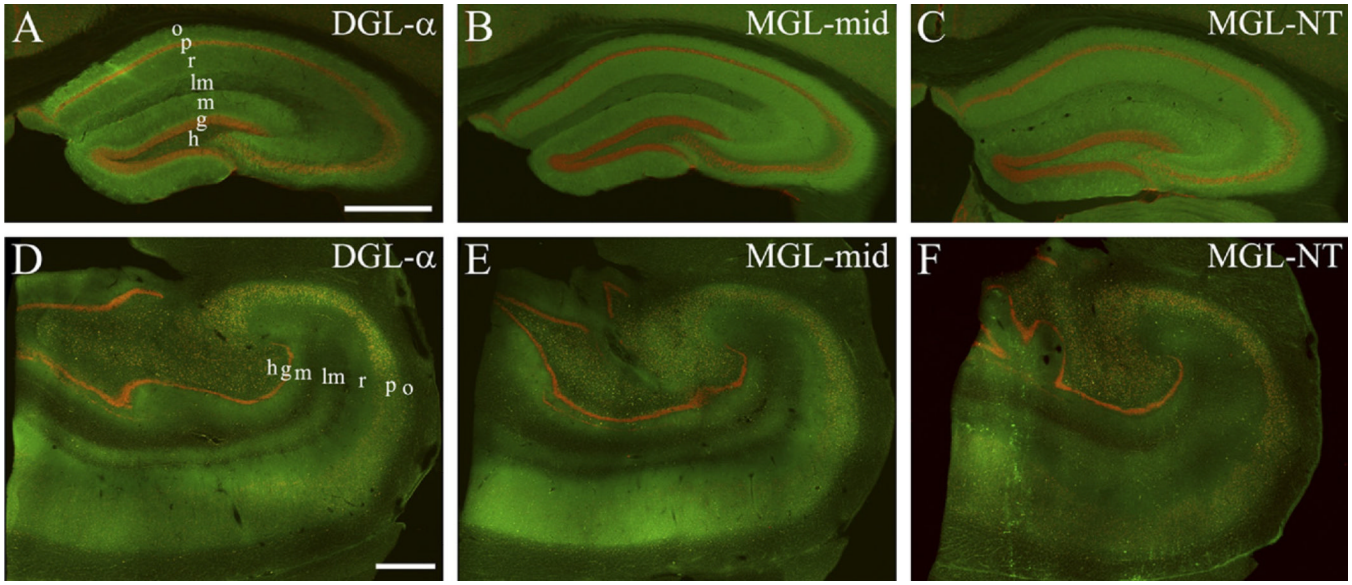

Fig. 2.

Comparable topographical distribution of 2-AG metabolizing enzymes in the mouse and human hippocampus. (A–C) Double immunofluorescence staining in the mouse hippocampus shows the laminar organization of DGL-α and MGL, responsible for generation and degradation of the endocannabinoid 2-AG, respectively (green). The cell bodies of neurons are visualized by NeuN staining (red) to highlight the pyramidal and granule cell layers. (D–F) A similar staining pattern is apparent in the human hippocampal formation. Note the laminar organization of the staining pattern for both enzymes indicating the spatial association of 2-AG metabolism with glutamatergic excitatory pathways. “MGL-mid” and “MGL-NT” indicates two distinct primary antibodies raised against different epitopes on the MGL protein. “MGL-mid” gives rise to denser immunostaining in the human hippocampus, whereas “MGL-NT” results in somewhat stronger staining in the mouse hippocampus. Nevertheless, both antibodies reveal comparable overall distribution of MGL in the mouse and human hippocampal formation. Abbreviations: o, stratum oriens; p, stratum pyramidale; r, stratum radiatum; lm, stratum lacunosum-moleculare; m, stratum moleculare; g, stratum granulosum; h, hilus. Scale bars: (A) 0.5 mm also applies to (B–C); (D) 1 mm also applies to (E–F).

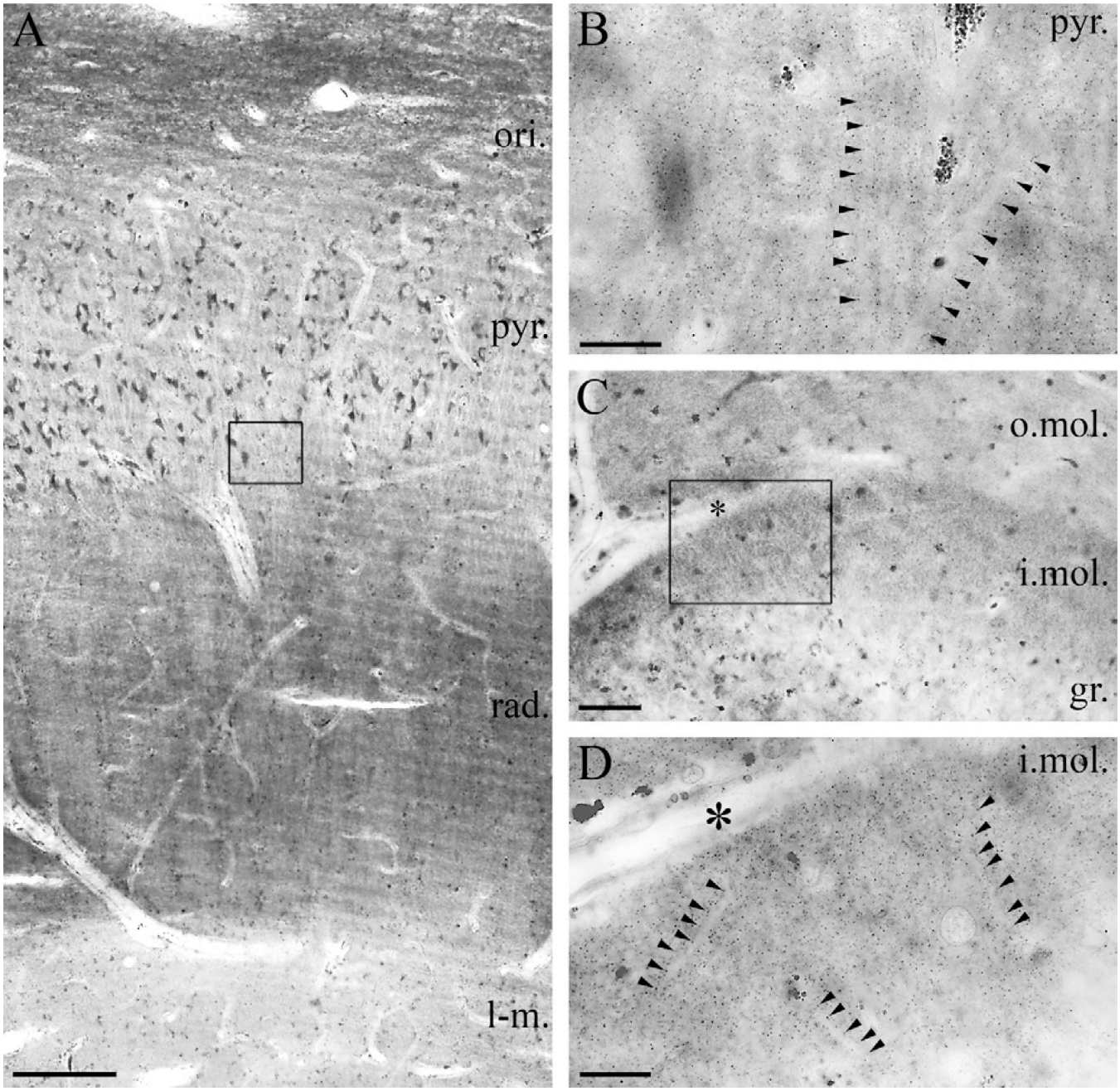

Fig. 3.

Light microscopic localization of DGL-α in the human hippocampus. (A) Light micrograph of DGL-α immunoperoxidase reactivity in the CA1 subfield of the cornu ammonis using the "DGL-α-INT" antibody. The highest density of immunostaining is located in the strata oriens (ori.) and radiatum (rad.), whereas staining intensity is somewhat weaker in the strata lacunosum-moleculare (l-m.) and pyramidale (pyr.). Besides the specific DGL-α immunoreactivity, lipofuscin granules in the cell bodies of pyramidal cells are also observed occasionally, but its relation to DGL-α protein was not considered, because these pigment granules are known to accumulate in neuronal somata during aging. (B) At higher magnification, the main apical dendrites of CA1 pyramidal cells at the border of stratum pyramidale and stratum radiatum appear to be DGL-α immunonegative and are contoured

by an intense dotted staining in the neuropil (arrowheads). (C) In the dentate gyrus, the highest density of DGL-α immunostaining is visible in the inner third of stratum moleculare (i.mol.), where the mossy cells, a glutamatergic interneuron type of the dentate gyrus terminate. Modest staining is observable in the outer two-thirds of stratum moleculare (o.mol), whereas immunolabelling was weak in stratum granulosum (gr.). (D) At higher magnification, immunonegative dendrites of granule cells are surrounded by widespread punctate DGL-α immunoreactivity (arrowheads) in inner third of the stratum moleculare of dentate gyrus. Open boxes denote the positions of corresponding insets (B in A, D in C). Asterisks in (C–D) depicts the same capillary used as landmark. Scale bars: (A) 200 μm; (B, D) 20 μm; (C) 50 μm.

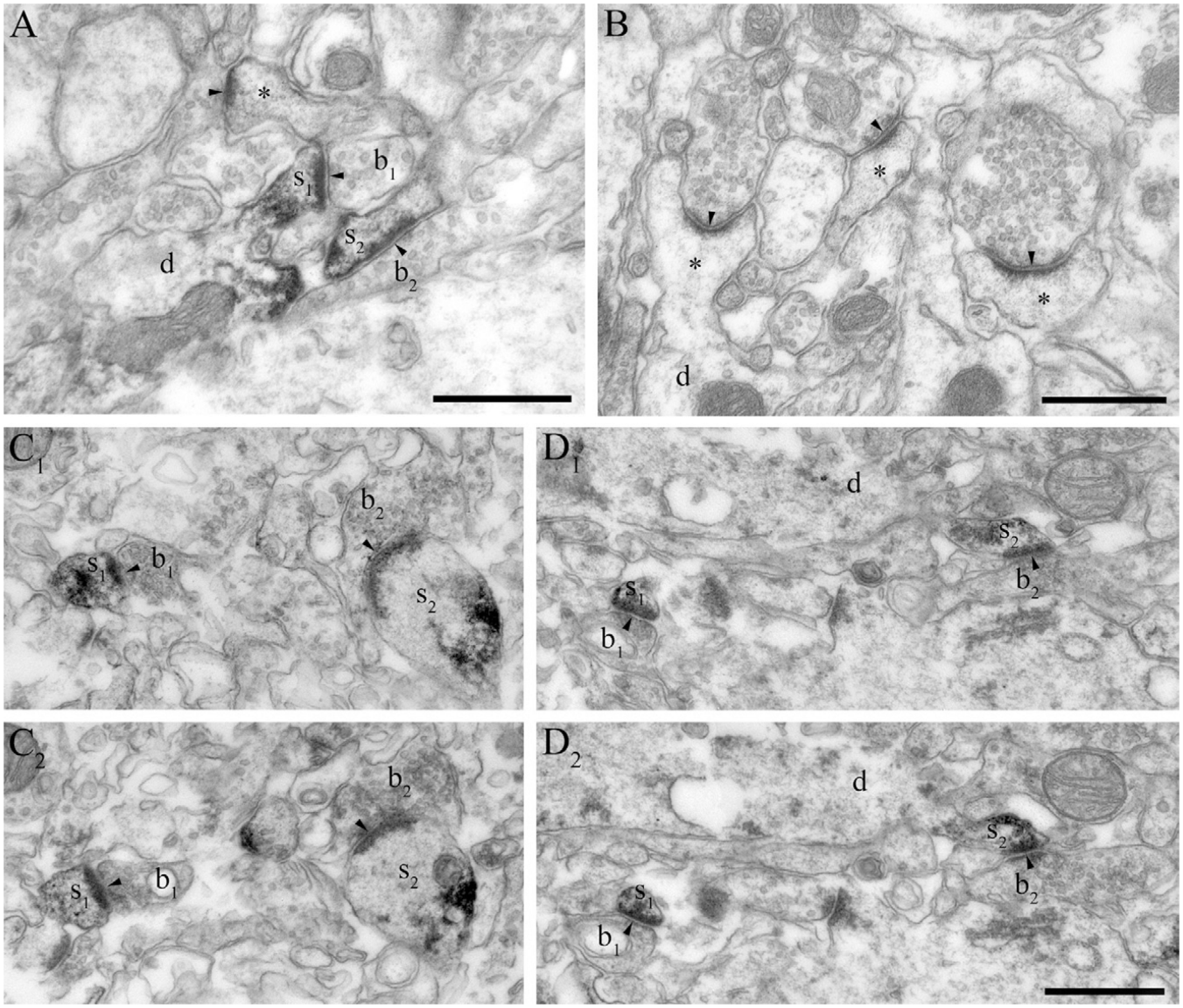

Fig. 4.

DGL-α is localized in dendritic spines in the mouse and human hippocampus. (A) Immunoperoxidase reaction performed on hippocampal sections derived from wild-type mice reveals that DGL-α is present in numerous dendritic spine heads (s_1–s_2) receiving asymmetric synapses (arrowheads) in the stratum radiatum of the CA1 subfield. These DGL-α immunopositive spines protrude from DGL-α immunonegative dendritic shafts (d). Other subcellular profiles like excitatory axon terminals (b_1–b_2) or other dendritic spines (asterisk) are also DGL-α immunonegative, which reflects that this enzyme is either absent or its level is under detection threshold in these compartments. (B) In hippocampal sections derived from DGL-α knockout animals, dendritic spines (asterisks) as well as other subcellular profiles (e.g. dendritic shafts depicted by "d") are all devoid of DGL-α immunoreactivity confirming the specificity of the antibody for DGL-α. (C_1–C_2) Serial high-resolution electron micrographs of DGL-α immunoreactivity in the stratum radiatum of the CA1 region in the human hippocampus. The black immunoreaction end-product DAB, representing the localization site of DGL-α, is accumulated in the dendritic spine heads (s_1–s_2) of CA1 pyramidal neurons. In contrast, DGL-α immunoreactivity levels did

not reach detection threshold in presynaptic axon terminals (b_1–b_2) forming asymmetric synapses (arrowheads) on the spine heads. (D_1–D_2) Similar situation is found in the inner third of stratum moleculare of the human dentate gyrus. The striking targeting of DGL-α to the postsynaptic side of excitatory synapses (arrowheads) is highlighted by the dense labeling in spine heads (s_1–s_2), which are derived from DGL-α immunonegative dendritic shafts (d) of granule cells. Other subcellular domains, e.g. axon terminals (b_1–b_2) are also devoid of DGL-α. Scale bars: (A, B, D_2) 500 nm, (D_2) also applies to (C_1, C_2, D_1).

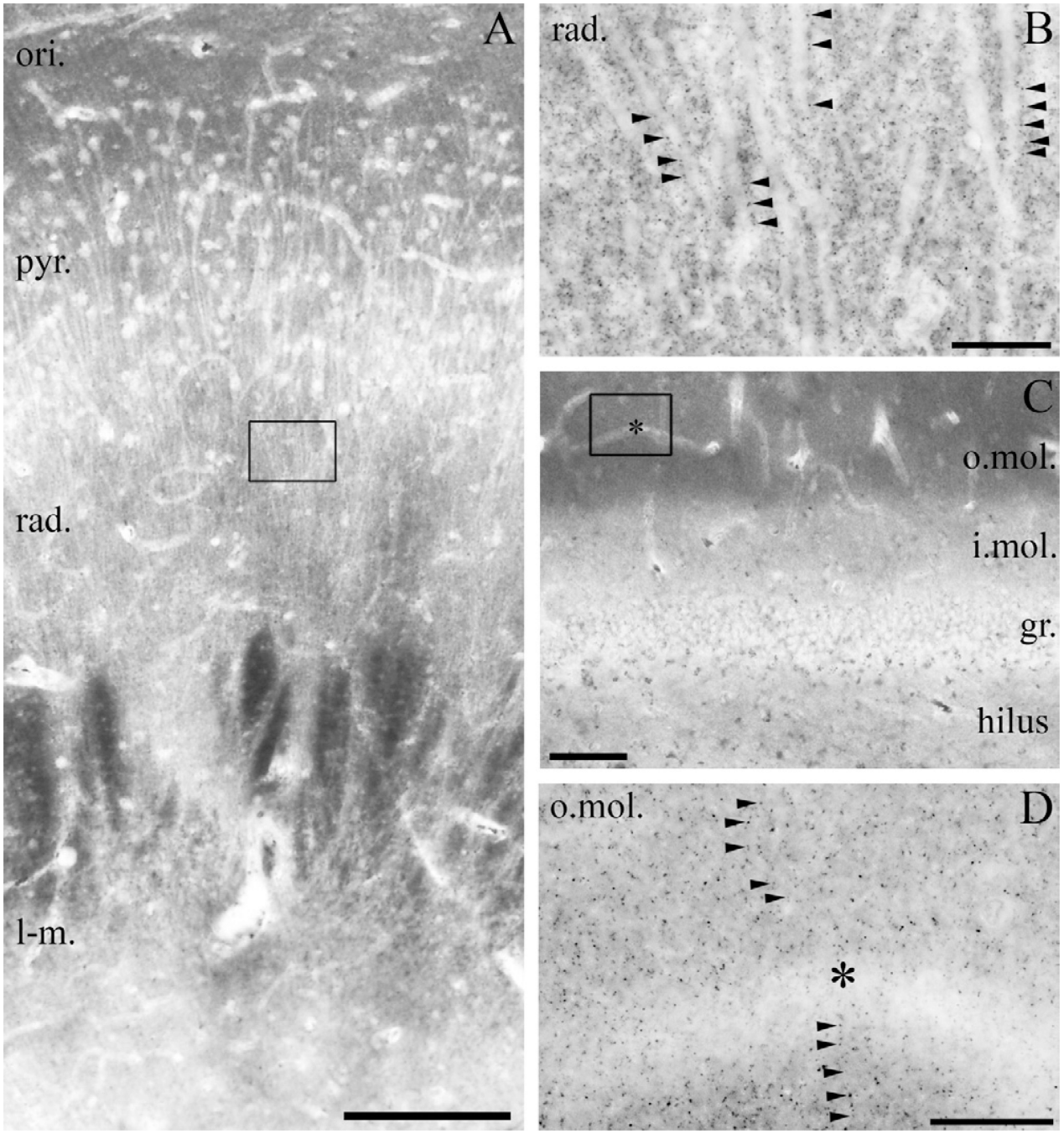

Fig. 5.

Light microscopic localization of MGL in the human hippocampus. (A) Light micrograph of immunoperoxidase staining for MGL in the CA1 subfield of the cornu ammonis shows that the highest density of MGL-immunoreactivity using the “MGL-mid” antibody is located in the stratum oriens (ori.), but significant levels of immunostaining is also apparent in strata pyramidale (pyr.), radiatum (rad.) and lacunosum-moleculare (l-m.). (B) At higher magnification, the abundant neuropil staining becomes visible, e.g. in the stratum radiatum of CA1 region (depicted here). The characteristic MGL-immunopositive granules (arrowheads) decorate MGL-immunonegative apical dendrites of pyramidal cells. (C) In the dentate gyrus, MGL-immunostaining was observed predominantly in the outer two thirds of

the stratum moleculare (o.mol.), whereas it was weaker in the inner third of stratum moleculare (i. mol.), stratum granulosum (gr.) and in the hilus. Somata of granule cells (similarly to somata of pyramidal cells in A) are hardly or not at all labeled by MGL immunostaining. (D) At higher magnification, the punctate neuropil staining is present throughout the stratum moleculare of the dentate gyrus. MGL-immunonegative dendrites are frequently outlined by the characteristic MGL-containing varicosities often arranged in an array-like manner. Open boxes denote the positions of corresponding insets (B in A, D in C). Asterisks in (C–D) depicts the same capillary used as landmark. Scale bars: (A) 200 μm; (B, D) 20 μm; (C) 100 μm.

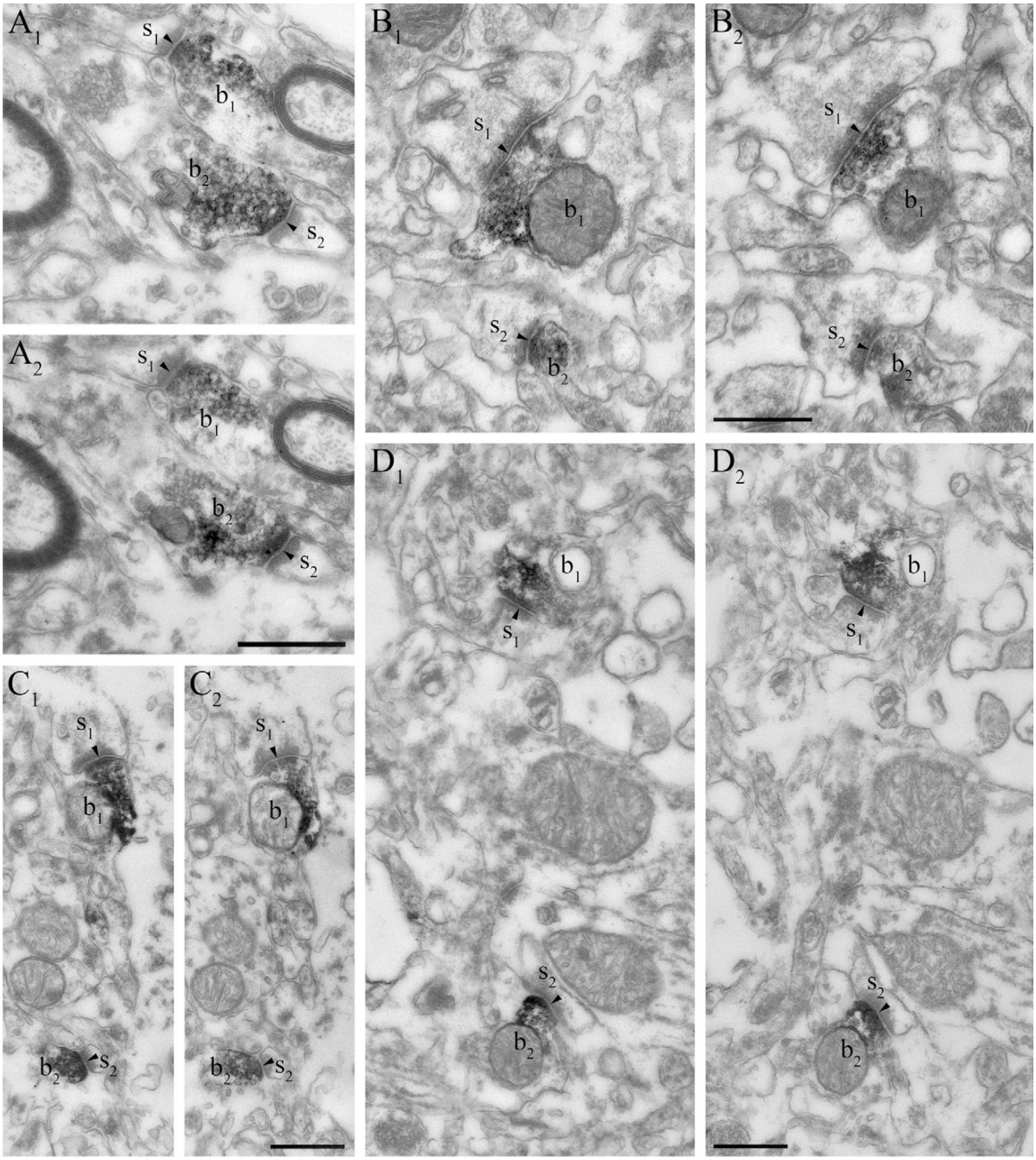

Fig. 6.

MGL is located presynaptically on glutamatergic axon terminals in the human hippocampus. (A_1–D_2) At the electron microscopic level, immunostaining with two independent antibodies raised against different epitopes of the MGL protein reveals the abundance of MGL in axon terminals forming asymmetric, presumably excitatory synapses (arrowheads). The antibody "MGL-mid" is used in (A_1–A_2) and in (C_1–C_2), whereas the antibody "MGL-NT" is used in (B_1–B_2) and in (D_1–D_2). Series of consecutive ultrathin sections show that the black DAB end product fills the intracellular side of the boutons (b_1–b_2, all images are two consecutive sections) indicating high levels of MGL enzyme in these axon terminals. Importantly, MGL-immunoreactivity levels did not reach detection threshold in spine heads,

in dendritic or in glial processes, and in cell bodies. The illustrated boutons are derived from the stratum radiatum in the CA1 region (b_1–b_2 in A_1–A_2 and B_1–B_2), and from the outer two thirds of stratum moleculare in the dentate gyrus (b_1–b_2 in C_1–C_2 and D_1–D_2). Scale bars: (shown in A_2, B_2, C_2, D_2) 500 nm, (also applies to A_1, B_1, C_1, D_1, respectively).